

ELECTRONIC SUPPLEMENTARY INFORMATION FOR

## Microfabricated Passive Vapor Preconcentrator/Injector Designed for Microscale Gas Chromatography

Jung Hwan Seo,<sup>ab</sup> Sun Kyu Kim,<sup>ad</sup> Edward T. Zellers,<sup>\*ade</sup> Katsuo Kurabayashi<sup>\*abc</sup>

<sup>a</sup> Engineering Research Center for Wireless Integrated Microsensing and Systems (WIMS),  
University of Michigan, Ann Arbor, MI 48109, USA

<sup>b</sup> Department of Mechanical Engineering, University of Michigan, Ann Arbor, MI 48109, USA.  
E-mail: katsuo@umich.edu; Fax: +1-734-647-3170; Tel: 1-734-615-5211

<sup>c</sup> Department of Electrical Engineering and Computer Science, University of Michigan, Ann  
Arbor, MI 48109, USA

<sup>d</sup> Department of Environmental Health Sciences, University of Michigan, Ann Arbor, MI  
48109, USA E-mail: ezellers@umich.edu; Fax: 734-763-8095; Tel: 734-936-0766

<sup>e</sup> Department of Chemistry, University of Michigan, Ann Arbor, MI 48109, USA

### Concept of Characteristic Length

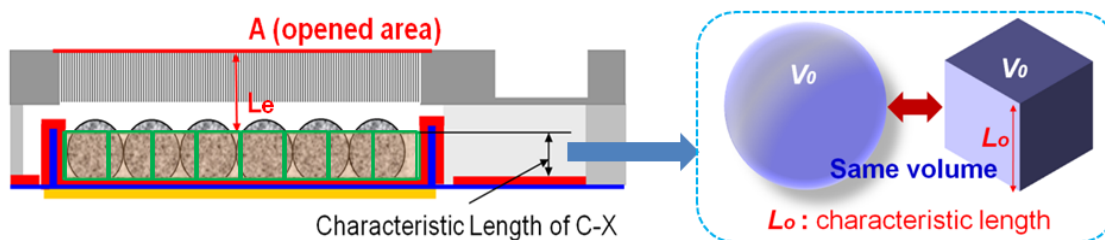


**Figure S1.** Diagrams illustrating the concept of the ‘characteristic length’ as it relates to estimating the sampling rate,  $S$ , of the  $\mu$ PPI. Here, the effective diffusion channel,  $L_e$ , is defined as the distance from the top entrance of the diffusion channel to the top surface of the C-X adsorbent layer. The C-X granules are assumed to be spherical, and they are modeled as cubes of equivalent volume. We define the characteristic length as the height (side) of the cube of the C-X granule:  $L_0$ . The value of  $L_0$  is determined from the average diameter of the C-X particle  $r_0$ , estimated from sieved fraction of C-X loaded into the device as  $\sim 200 \mu\text{m}$ . The corresponding characteristic length is  $L_0 = V_0^{1/3} = (4\pi/3)^{1/3} r_0 = 161 \mu\text{m}$ . The effective

diffusion length,  $L_e = L_1 + L_2 = 265 \mu\text{m}$  (see below and main article for definitions of  $L_1$  and  $L_2$ ), is obtained by subtracting  $L_0 = 161 \mu\text{m}$  from the distance from the cavity floor to the top entrance of the diffusion channel ( $= 426 \mu\text{m}$ ).

### Derivation of Effective Sampling Rate, $S_e$

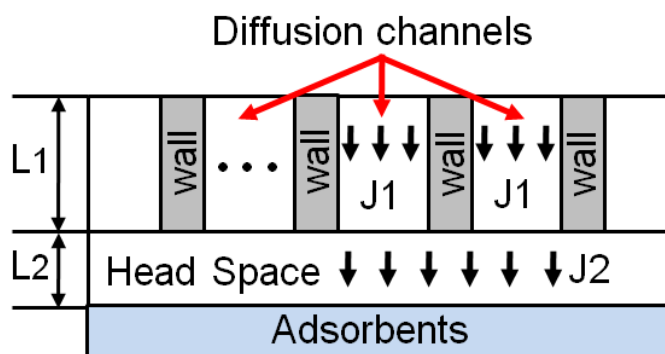


**Figure S2.** Cross-sectional view of the  $\mu\text{PPI}$  structure consisting of the diffusion channel array, head space, and the C-X adsorbent layer.

From the 1D diffusion equation and Fick's law, the sampling rate for a diffusion channel is derived as:

$$j = -D \frac{dC}{dZ} = D \frac{\Delta C}{L} = \frac{M}{A \cdot t} \quad (\text{Eq. S1})$$

where  $j$  is the vapor flux,  $D$  is the vapor diffusion coefficient,  $\Delta C$  is the concentration difference between two positions along the diffusion path,  $L$  is the diffusion length,  $M$  is the vapor mass (or alternatively, the number of molecules),  $A$  is the cross sectional area normal to the diffusion direction,  $t$  is the sampling period. It follows that the sampling rate  $S$  is given by

$$S = D \frac{A}{L} = \frac{M}{\Delta C \cdot t} \quad (\text{Eq. S2})$$

From Eq. S1 and Eq. S2, the mass flow rate  $J$  is expressed as:

$$J = (\Delta C)S \quad (\text{Eq. S3})$$

The vapor flow driven by diffusion takes place inside the device through two regions: (a) the diffusion channel layer and (b) the head space. Applying the mass conservation rule to the above two regions, we obtain the following equations.

$$J = (C_1 - C_i)S_1 = (C_i - C_2)S_2 \equiv (C_1 - C_2)S_e \quad (\text{Eq. S4})$$

where  $C_1$  is the vapor concentration at the top surface of the diffusion channel layer of thickness  $L_1$  and total diffusion cross sectional area  $A_1$ ,  $C_i$  is the vapor concentration at the interface between the diffusion channel layer and the head space of height  $L_2$  and cross sectional area  $A_2$ ,  $C_2$  is the concentration at the adsorbent surface,  $S_1 = D \frac{A_1}{L_1}$  is the sample flow rate through the diffusion channel layer,  $S_2 = D \frac{A_2}{L_2}$  is the sample flow rate through the head space, and  $S_e$  is the overall effective sample flow rate for the entire diffusion length ( $L_1 + L_2$ ). From Eq. S4, we obtain

$$S_e = \frac{S_1 S_2}{S_1 + S_2} = D \frac{A_1 A_2}{A_1 L_2 + A_2 L_1} \quad (\text{Eq. S5})$$

The sampling rate for each region can be calculated from Eq. 1 as  $S_1 = 11.4$  mL/min and  $S_2 = 52.1$  mL/min.  $A_1$  is  $4.5 \text{ mm}^2$  and the cross sectional area ( $A_2$ ) in the headspace is 49% larger than  $A_1$  due to the lack of diffusion grid walls. From Eq. S5, the overall effective sampling rate  $S_e$  is 9.3 mL/min.

### Modeling Gas Flow Dynamics

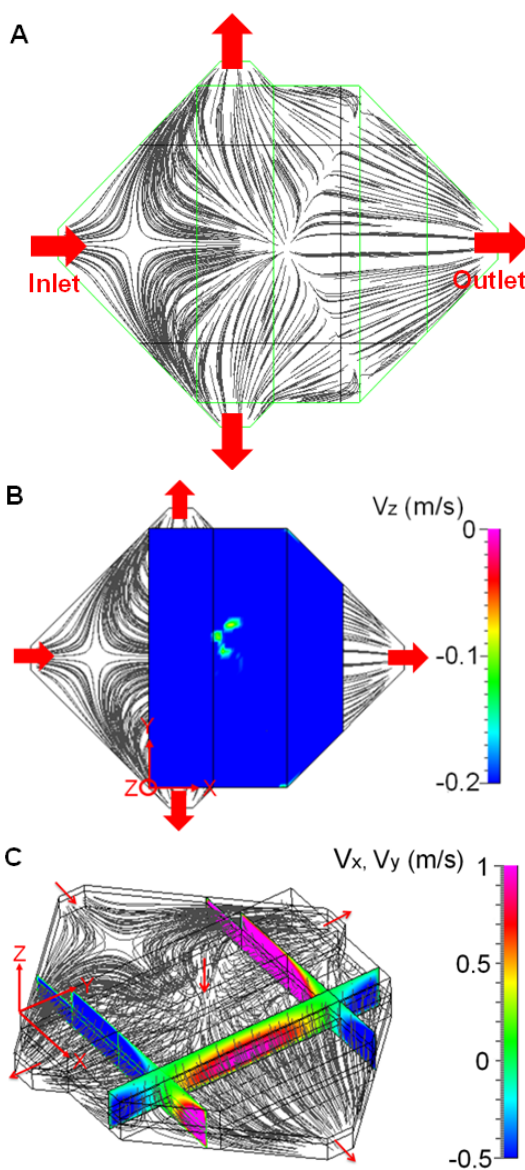


**Figure S3.** (A) Velocity field of desorbed vapors in a carrier gas flowing inside the cavity from the inlet and the top diffusion channels, divided into three regions close to the outlets. (B) Computational fluid dynamics analysis of the vertical (z-direction) velocity of the vapor flow at the top surface of the diffusion channels (colored) with suction pressure applied to the outlets. (C) Vapor flow patterns inside the device cavity and distribution of velocity magnitude at vertical cross sections (normal to the outlet flows).

Upon heating the device membrane, vapor molecules desorbed from the adsorbent materials might escape through the diffusion channels due to the developed concentration gradient in the vertical direction. To understand how the carrier gas flow dynamics affect the potential for sample loss during the suction process, we performed computational fluid dynamics (CFD) analysis of the designed  $\mu$ PPI device. Results show that all thermally desorbed vapors migrate to the outlets without escaping through the diffusion channels. The red arrows in Fig. S3A indicate the flow direction at the inlets (including diffusion channels) and outlets. The CFD model numerically solves the full Navier-Stokes equations assuming Newtonian incompressible flow in the cavity chamber. It predicts the relatively complex flow pattern of the vapor molecules in a carrier gas in either the laminar or turbulent regime. The heater temperature and the suction pressure at the outlet are both programmable and controllable. Thus, all boundary conditions are determined according to the operational conditions of our choice. The initial pressure of the inlet is set at ambient pressure here. The pressure drop at the outlet, provided by a mini diaphragm pump, is assumed to be 15 kPa. The ambient temperature and the temperature of the cavity floor upon desorption are set at 25°C and 300°C, respectively.

The CFD analysis considered the worst-case condition that would yield the maximum vapor loss and the lowest vapor flow rate at a given pressure drop. The condition is realized when the analysis assumes that the cavity is empty (i.e., there is no adsorbent), which is verified by the model in Fig. S6. In the real device setting, the volume of the adsorbents filling the cavity reduces the effective cross-sectional area through which the vapor is horizontally carried during the sample injection process. This real condition results in higher horizontal ( $x$ -direction) vapor velocity, and hence less vapor losses at the same pressure drop as used in the analysis. Assuming a spherical adsorbent granules, the vapor desorption rate of 34.0 mL/min, which was calculated for the overall cavity area using Eq. 2 and Eq. 3 in the

main text, is converted to a linear velocity of 0.1 m/sec emanating radially from each adsorbent granule. The average desorption linear velocity projected in the vertical ( $z$ -) direction is 0.07 m/sec; a value that represents a true boundary condition in the vertical direction from the bed of adsorbents packed within the cavity. To be conservative in our prediction, we applied a vapor desorption linear velocity of 0.12 m/sec in the vertical direction as the boundary condition from the bottom chamber floor.

Figures S3B and C show the prediction of the net vertical ( $z$ -direction) velocity of the vapor in the carrier gas, accounting for the counter flow of vapor by diffusion at the desorption temperature. Our simulation indicates that the carrier gas will pass through the entire open area of the diffusion channel grid and will be collected by the outlets without vapor loss. It also shows no vortices or stagnation points inside the cavity. A suction flow rate of 60 mL/min ensures that the  $z$ -direction velocities of the carrier gas have negative values over the whole area at the top surface of the diffusion channel grid. Under this condition, it is expected that the desorbed vapor molecules are effectively captured by the carrier gas and drawn out through the outlet ports. Therefore, we employed the 3-outlet design as the optimal passive preconcentrator design in our study.

## Fabrication Process

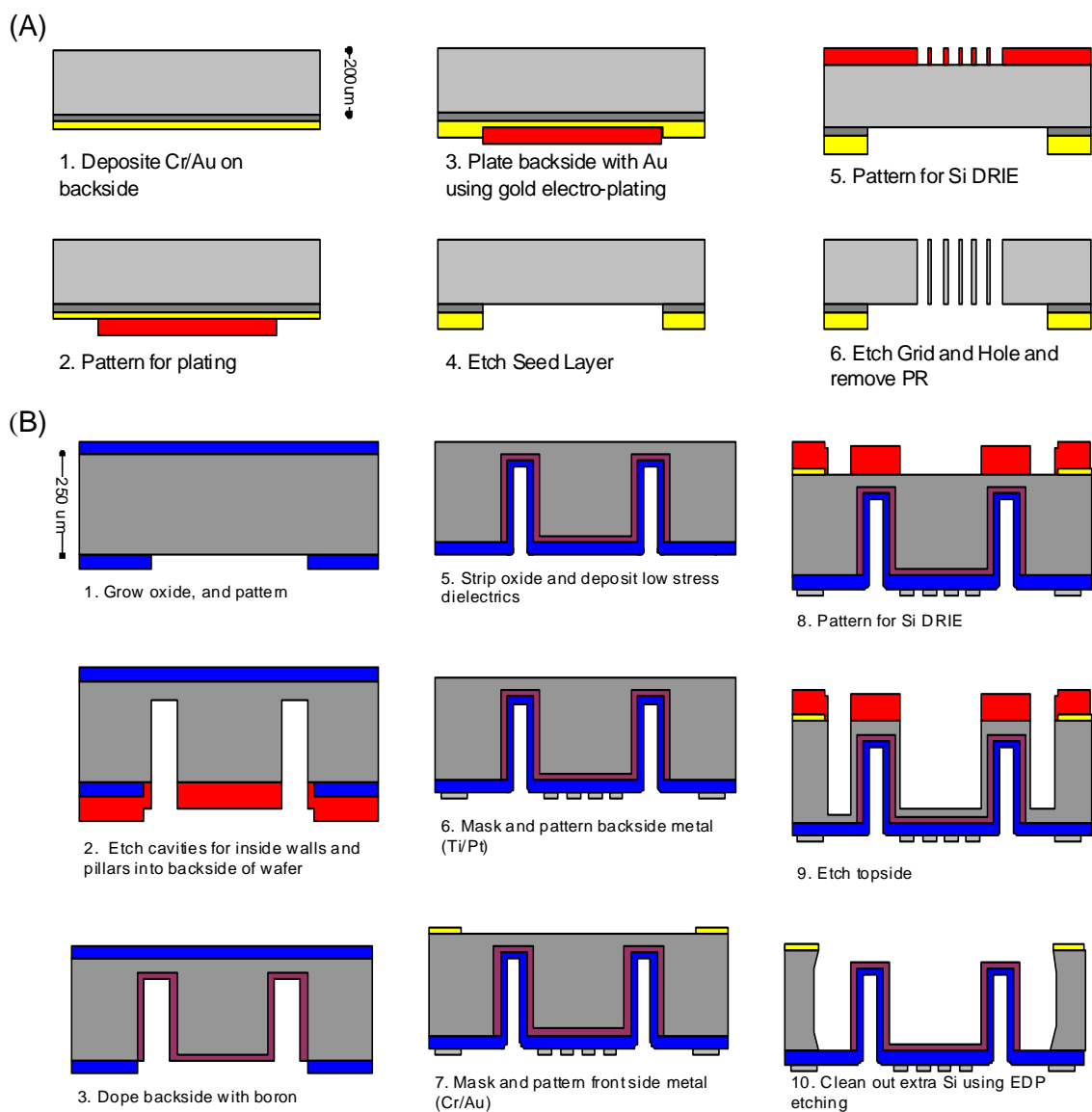


**Figure S4.** Device fabrication process steps for (A) top layer and (B) bottom layer Fabrication processes

### Thermal Response Profiles

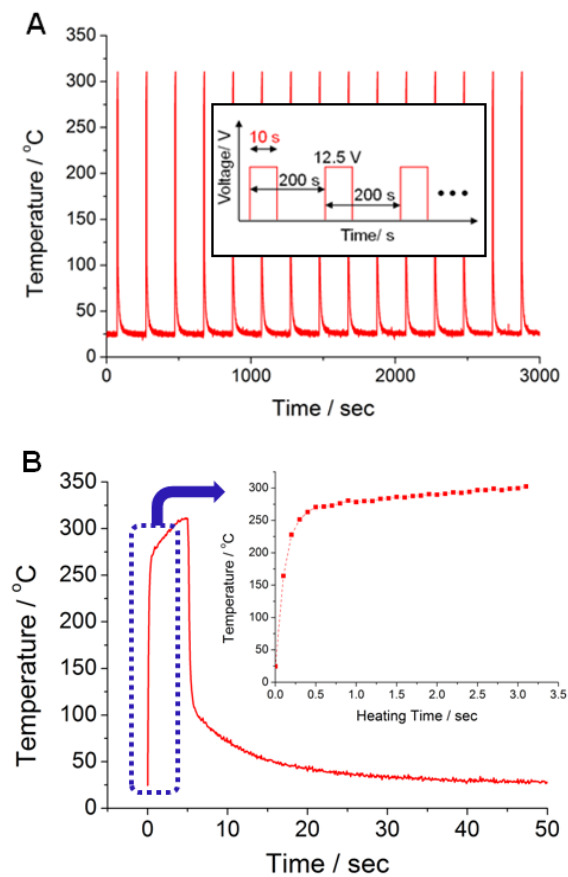


**Figure S5.** Thermal response of the  $\mu$ PPI at power input of  $\sim 1$ W. (A) Temperature profile of the  $\mu$ PPI cavity membrane during thermal cycling. Each cycle with a 200 s period consists of a heating cycle of 10 s and a cooling cycle of 190 s. (B) Magnified temperature profile of the  $\mu$ PPI cavity membrane during the heating cycle. The temperature reaches 250 °C in 0.23 sec and 300 °C in 3 sec.

### Minimum Flow Rate for Quantitative Transfer/Injection

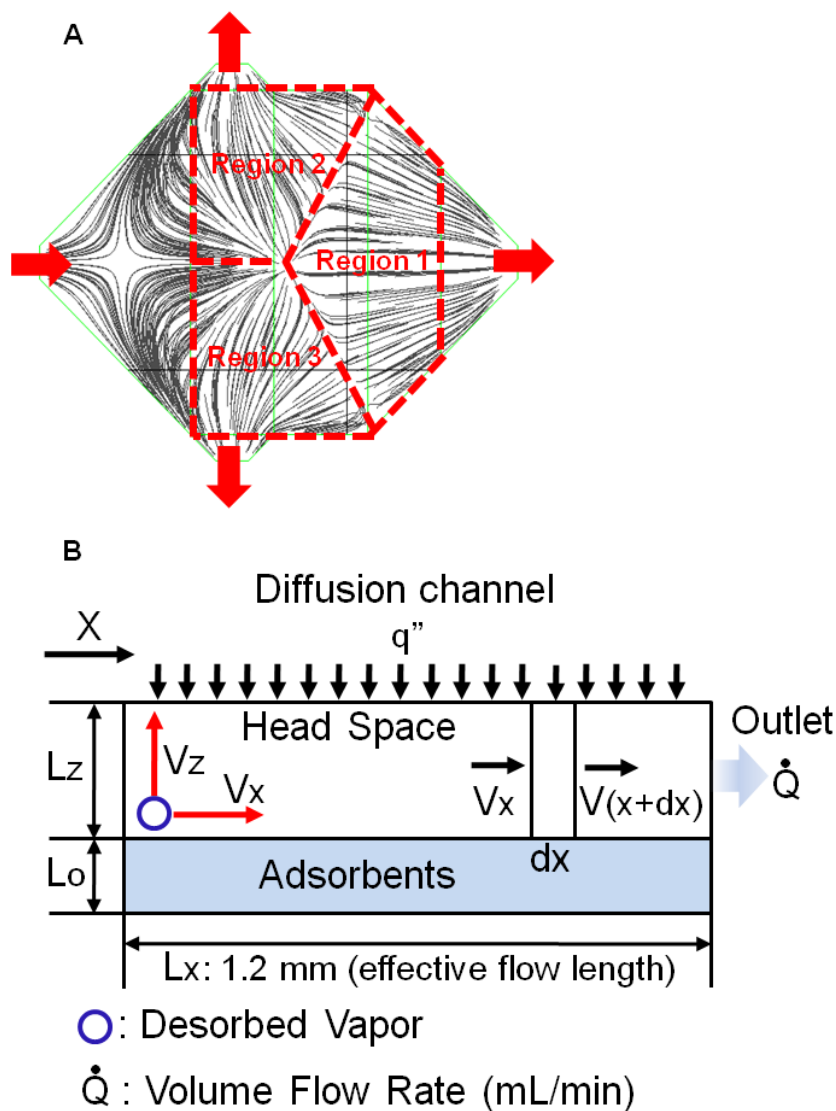


**Figure S6.** (A) Top view of characteristic flow regions within the  $\mu$ PPI cavity. (B) Simplified cross-sectional view of a characteristic flow region of the  $\mu$ PPI cavity, which is used in the model for predicting the capture/transfer efficiency as a function of the suction flow rate, as shown in Fig. 6 in the main article. The model allows us to examine the "no vapor loss condition" for the empty cavity condition ( $L_0=0$ , maximum head space condition) and the adsorbent packed condition ( $L_0=161 \mu\text{m}$ , minimum head space condition). These two cases

are studied to verify that the CFD model in Fig. S3 is the most conservative (i.e., the worst scenario) condition.

The CFD analysis indicates that the device cavity can be divided into 3 characteristic flow regions between the central node of the flow pattern and the 3 outlet positions (Fig. S3B), regardless of the suction flow rate. These regions have similar velocity distributions and flow streamline patterns. The top of each characteristic region represents a position at the bottom of the diffusion channel layer of the  $\mu$ PPI. A spatially uniform vapor flux  $q''$  driven by convection vertically enters the characteristic region from the top. The shape of each characteristic region is approximated as a rectangular box defined by the cavity height (the adsorbent height  $L_0$  + the head space height  $L_z$ ), the effective flow length  $L_x$ , and the characteristic width  $L_y$ . The values of  $L_x$  and  $L_y$  are determined by taking the average distance between the two facing sides of the frame delineating the characteristic region in the  $x$ -direction (i.e., the direction pointing towards the outlet from the central node) and  $y$ -direction (i.e., the direction normal to the  $x$ - $z$  plane), respectively. For Region 1,  $L_x$  is 1.2 mm and  $L_y$  is 2.0 mm, whereas  $L_x$  and  $L_y$  are both 1.2 mm for Regions 2 and 3.  $L_z$  is 89  $\mu$ m and 250  $\mu$ m for the adsorbent packed condition and the empty cavity condition, respectively.

The model derives a mathematical formulation which accounts for the fraction of the amount of vapor arriving at the bottom of the diffusion channel layer in the  $z$ -direction before reaching the outlet to the total amount of vapor leaving the C-X surfaces. The "no loss condition" refers to the condition where the desorbed vapors leaving the adsorbent surface should horizontally reach the outlet without vertically arriving at the bottom surface of the diffusion channel layer. The vapor velocity distribution is assumed to be uniform across the  $x$ - $y$  plane. The  $x$ -direction velocity  $V_x$  is estimated from the volumetric flow rate at each outlet. The vapor velocity to the  $z$ -direction  $V_z$  is equivalent to the vapor desorption linear velocity. The no loss condition requires the following relationship for the motion of the vapor

molecules leaving the adsorbent surface at the left-end corner at  $x=0$ :

$$t_x \leq t_z, \quad (\text{Eq. S7})$$

where  $t_x$  is the time required for the particle to pass through the cavity in the  $x$ -direction,  $t_z$  is the time required for the particle to reach the bottom of the diffusion channel layer in the  $z$ -direction. Applying mass balance for the differential control volume between  $x$  and  $x+dx$ , the governing equation for  $V_x$  is derived as

$$\frac{dV_x}{dx} - \frac{q''}{L_z} = 0, \quad (\text{Eq. S8})$$

Solving the equation with the boundary conditions:  $V_x(x=L_x) = q''(L_x + L_z)/L_z$ , and  $V_0 = q''$ , which are derived from conservation of mass for the entire cavity and from the Bernoulli equation, yields

$$V_x(x) = q'' \frac{(x + L_z)}{L_z} \quad (\text{Eq. S9})$$

Now, the horizontal travel time  $t_x$  and the vertical travel time  $t_z$  are given as follows:

$$t_x = \int_0^{L_x} \frac{1}{V_x} dx \quad (\text{Eq. S10})$$

$$t_z = \frac{L_z}{V_z} \quad (\text{Eq. S11})$$

Then, the critical position  $x_c$ , which is the position along the  $x$ -direction where  $t_x = t_z$  for the vapor molecules leaving the adsorbent surface, can be found using Eq. S10 and Eq. S11, yields

$$t_z = \int_{x_c}^{L_x} \frac{1}{V_x} dx \quad (\text{Eq. S12})$$

From Eq. S12, the critical position  $x_c$  can be determined for a given volumetric flow rate. The vapor molecules desorbed at  $0 < x < x_c$  escape from the diffusion channel while those desorbed at  $x > x_c$  are captured by the outlet flows and injected downstream from the  $\mu$ PPI.

Thus, the capture/transfer efficiency  $eff$  is given by

$$eff = \frac{L_x - x_c}{L_x} \times 100 \quad (\text{Eq. S13})$$

Using Eq. S13, the minimum volumetric flow rates satisfying the "no loss condition" are 58.7 mL/min and 50.1 mL/min for the empty cavity and the adsorbent-packed cavity, respectively. Therefore, we can conclude that the empty cavity (maximum head space case) represents the most conservative condition, leading to the maximum vapor loss. The flow rate value of 58.7 mL/min is consistent with that used in the aforementioned CFD analysis.